Electric Field-Induced Changes in Lipids Investigated by Modulated Excitation FTIR Spectroscopy

Michael Schwarzott,* Peter Lasch,† Dieter Baurecht,* Dieter Naumann,† and Urs Peter Fringeli*
*Institute of Physical Chemistry, University of Vienna, A-1090 Vienna, Austria; and †Robert Koch-Institut, 13533 Berlin, Germany

ABSTRACT The effect of electric fields on dry oriented multibilayers of dimyristoylphosphatidylcholine (DMPC) was investigated by transmission Fourier transform infrared electric field modulated excitation (E-ME) spectroscopy. A periodic rectangular electric potential (0–150 V, 1.25 Hz, 28.4°C ± 0.2°C) was applied across the sample. To discriminate electric field-induced effects from possible temperature-induced effects resulting from a current flow (<1 pA) across the sample, corresponding temperature-modulated excitation (T-ME) measurements within the temperature uncertainty limits of ±0.2°C at 28.4°C were performed. T-ME induced reversible *gauche* defects in the hydrocarbon chains, whereas E-ME resulted in reversible compression of dry DMPC bilayers. Periodic variation of the tilt angle of the hydrocarbon chains is suggested. The degree of absorbance modulation in the CH-stretching region was found to be in the order of 1:700, corresponding to a variation of the bilayer thickness of $\Delta z = 0.0054$ nm. Using a series connection of capacitors as equivalent circuit of the cell resulted in $E = (1.2 \pm 0.7) \times 10^7$ V/m for the electric field in DMPC. Young's elasticity modulus of DMPC could be calculated to be $E_\perp = 2.2 \times 10^6$ Pa $\pm 1.8 \times 10^6$ Pa, which is in good agreement with published data obtained by electric field-dependent capacitance measurements.

INTRODUCTION

Strong electric fields acting on lipid membranes influence the lipid structure and can even lead to a mechanical rupture (Winterthaler, 1999). This electric perturbation of lipids is used in technical applications as eletroporation and electrofusion, however, the underlying molecular mechanism has not been elucidated in detail so far. Information about mechanical, electrical, and dynamic properties of supported lipid bilayer membranes was found by various electrochemical methods, e.g., electrostriction and dielectric relaxation measurements (Hianik, 2000). Changes of the modulus of elasticity, the coefficient of dynamic viscosity, the membrane capacitance, and membrane potentials as well as dipole reorientations are reported. Information on a molecular structural base is available by infrared spectroscopic methods. The influence of strong electric fields on the structure of dry oriented membrane stacks composed of dioleylphosphatidylcholine or dimyristoylphosphatidylcholine (DMPC) containing the peptide melittin was investigated by attenuated total reflection (ATR) Fourier transform infrared (FTIR) spectroscopy (Le Saux et al., 2001). Both, the internal reflection element and the counterelectrode consisted of germanium, and were coated by a thin layer of polystyrene (165 nm) to avoid electrochemical processes in the assembly. It was found that melittin did not respond to the electric field in both lipids, however, prominent signals were detected of the polar headgroups of the lipids, especially of the phosphate and choline moieties. The presented results indicate, that 2–3% of the polar headgroups changes the orientation in such a way that the phosphate group and the N-$(CH_3)_3$ moiety adopt a more perpendicular orientation to the membrane surface. Most astonishingly, no field-induced effects were observed in the spectral regions of the hydrocarbon chains. More recently, Sargent (2001) commented on the findings of Le Saux et al. (2001) in a letter to the editor, pointing out that voltage jump/capacitance relaxation studies (Sargent, 1975a,b) performed with black lipid membranes as well as with solvent free lipid bilayers (Hianik et. al., 2000) support the finding of electric field induced conformational changes in the polar headgroup region. However, based on the very high sensitivity achievable with displacement current measurements, Sargent (2001) concluded that the realignment of the polar headgroup from approximately parallel orientation to the membrane surface toward the membrane normal was in the order of only 1° per 100 mV of potential change across a bilayer. Based on the experimental conditions used by Le Saux et al. (2001), Sargent (2001) estimated that the average potential drop across the bilayers on the ATR plate was at the most a few hundred mV per bilayer. This means, that the angular amplitude of the field-induced movement of the polar headgroup should be expected within a few degrees only.

Our approach to the study of electric field-induced conformational changes in model biomembranes is based on the application of the more advanced modulated excitation (ME) technique in the FTIR ATR and transmission mode. ME spectroscopy results in utmost sensitivity and time-resolved information, provided the sample of interest admits a periodic excitation by the modulation of an external parameter, such as the electric field (Fringeli et al., 2000; Baurecht and Fringeli, 2001; Baurecht et al., 2002).

Submitted January 21, 2003, and accepted for publication September 2, 2003.

Address reprint requests to Urs Peter Fringeli, Institute of Physical Chemistry, University of Vienna, Althanstrasse 14, A-1090 Vienna, Austria. Tel.: +43-1-4277-525-30; Fax: +43-1-4277-9525; E-mail: urs.peter.fringeli@univie.ac.at.

0006-3495/04/01/285/11 $2.00

In the present study we report on first results obtained by FTIR ME transmission spectroscopy, using dry oriented DMPC multilayers. Our membrane assembly was similar to that used by Le Saux et al. (2001) and Hianik (2000).

MATERIAL AND METHODS

Materials

DMPC (~98%, Sigma, St. Louis, MO) was suspended in distilled water (5.96 mg/mL) and exposed to ultrasonic treatment for ~10 min. A drop of 10 μL was disposed on the free aperture of one Si/SiO_2 window of the transmission cell and dried in a weak stream of air. Such an assembly was estimated to consist of ~500 DMPC bilayers on the mean.

Experimental setup

The transmission cell was built up of two cylindrical Si windows (20 mm in diameter and 2 mm thick) separated by a 5-μm polytetrafluorethylene (PTFE (Teflon), Goodfellow, Huntington, England) spacer as shown schematically in Fig. 1.

The inner surface of the Si windows were chemically etched to get an electrically insulating SiO_2 layer of ~200 nm (Micro-Biolytics GmbH, Freiburg, Germany). Electrical contact to Si was established by means of a silver foil pressed against the windows by the frame of the transmission cell. Temperature control to keep 28.4°C ± 0.2°C was achieved by water circulating from a thermostat through aluminum plates mounted on either outer side of the cell. The temperature was measured by a thermocouple fixed in the cell frame close to the Si window. The transmission cell had a free circular aperture of 7 mm diameter and was mounted on a rotatable shuttle platform, allowing a computer controlled displacement from the infrared (IR) beam to measure background spectra, as well as a change of the angle of incidence of the IR beam within $\varphi = 0°$ and $\varphi = 45°$ by rotation. The rotation axis of the cell was normal to the direction of propagation of the IR beam and normal to the horizontal platform. Electrical stimulation by a rectangular unipolar signal $U_{applied}$ (0–150 V) of 1.25 Hz, corresponding to a period of 0.8 s, was produced (Fig. 1) by switching a DC voltage source on and off under the control of the computer of the IR spectrometer. Potential generation was performed by a low-voltage DC source (Tabor, Model 8024, Unterschleißheim, Germany) that was amplified by a bipolar amplifier (BOP 500M, Kepco Inc., Flushing, NY) to a high voltage (150 V). In the potential free half-cycle of 0.4 s the cell capacitance was discharged by connecting the two windows via a 30 kΩ resistor. The steady-state potential profile across the four dielectric layers between the Si windows was calculated by means of Eq. 1, which is derived assuming an equivalent circuit of four capacitors connected in series.

$$E_k = \frac{U_{applied}}{\sum_{i=1}^{n} \frac{\varepsilon_k}{\varepsilon_i} d_i}, \quad (1)$$

where n is the number of dielectric layers, ε_i is the relative permittivity (dielectric constant), and d_i denotes the thickness of the i dielectric layer.

The relevant data are summarized in Table 1 and field profile is shown in Fig. 2.

Modulation excitation measurement

The application of modulated excitation techniques in FTIR spectroscopy may encounter fundamental problems due to interference of the external excitation frequency ω with frequencies of the interferogram. In case of slow modulations, i.e., the period of stimulation τ is in the range of one second or longer, this problem can be avoided by the application of a new technique, referred to as vector phase sensitive detection (PSD) (Fringeli, 1997; Baurecht and Fringeli, 2001). The novelty of this method was that FTIR spectra were treated as if they were points of a periodic signal response of a stimulated system. To do that, 16 equidistant time-resolved single channel spectra, referred to as sample-point spectra, (one scan per spectrum in this application) were recorded within each period of stimulation. Thus eight sample-point spectra were associated with the half-period, while the potential was applied to the cell and the second eight sample-point spectra were recorded in the half-period where the potential was switched off. Such cycles were repeated 3000–6000 times, simultaneously co-adding corresponding sample-point spectra. The duration of an excitation period was therefore determined by the scanning velocity of the interferometer that was set to 8.86 cm/s (laser modulation frequency of 280 kHz), as well as by the number of sample-point spectra ($n = 16$) and the number of scans per sample-point spectrum ($N = 1$).

During the application of constant potentials up to 150 V no DC current across the cell could be detected by our electrometer (Keithley 6517, Keithley Instruments, Cleveland, Ohio) featuring a sensitivity of 1 pA. Nevertheless considerable attention was made to unambiguously proof that potential-induced spectral changes did not result from periodic sample heating by a current <1 pA. Temperature was controlled to 28.4° ± 0.2°C by circulating water from a thermostat through heat exchanger plates screwed to either side of the transmission cell.

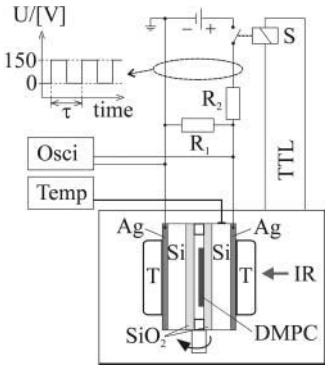

FIGURE 1 Schematic description of the experimental setup used for modulated excitation (ME) FTIR transmission measurements. The transmission cell consisted of two silicon (Si) windows coated at the inner sides by electrically isolating thin layers of silicon dioxide (SiO_2). The windows were separated by a 5-μm PTFE spacer. A drop of DMPC suspended in distilled water was dried on one Si window leading to a well-ordered assembly of ~500 bilayers. This window was connected to the positive pole of the electric source. Electric contact was achieved by means of silver foils (Ag) at the outer side of each window. The temperature was measured with a thermocouple (Temp), which was in contact with a Si window. The potential versus time course was displayed on an oscilloscope (Osci). The transmission cell enabled rotation (see *arrow*) to achieve angles of incidence within $\varphi = 0°$ and 45°. The incident infrared (IR) light was polarized. The plane of incidence was determined by the direction of light propagation and the normal to the cell windows at oblique incidence, which means $\varphi > 0°$. A rectangular modulated electrical potential varying between 0 and 150 V was used for electric field modulated excitation. The time-per-scan of the moving mirror of the interferometer was used as time unit for data acquisition. Sixteen scans resulted in one period of $\tau = 0.8$ s duration corresponding to 1.25 Hz. Always after eight scans the relay (S) was switched alternatively on and off, controlled by a TTL signal produced in the spectrometer, thus connecting the cell periodically to the stimulating potential. Two resistors $R_2 = 50\ \Omega$ in series and $R_1 = 30\ k\Omega$ parallel to the cell, enabled discharging of the cell in the potential-free half-phase. For temperature-modulated excitation the TTL signal of the computer was used to trigger a valve switching, resulting in alternative connection of the cell thermostatization plates (T) to two water circulation thermostats kept at different temperature.

TABLE 1 Summary of dielectric constants and thicknesses of the layers as presented by Fig. 2

	Relative permittivity (dielectric constant) of the k-th dielectric layer, $\varepsilon_{r,k}$	Thickness d_k of the k-th dielectric layer [μm]	Electric field, E_k [V/m]	Electric potential $\Delta U_k = U_{initial} - U_{final}$ [V]
SiO_2	4.3 ± 0.3*	0.2 ± 0.1	1.1 ± 0.1 × 10^7	1st layer:150 − 147.8 2nd layer: 2.2 − 0
DMPC	4 ± 2†	2.5 ± 1	1.2 ± 0.7 × 10^7	147.8 − 118.7
Air	1 ± 0*	2.5 ± 1	4.7 ± 2 × 10^7	118.7 − 2.2

Stationary electric fields within the layers were calculated by means of Eq. 1. The corresponding potential difference across the k-th layer, $\Delta U_k = E_k \times d_k$ is also indicated in Table 1 and plotted in Fig. 2.

*From Handbook of Chemistry and Physics 1974–1975

†Mean value derived from: *ε(hydrocarbon layer) = 2, ε(polar headgroups) = 8 (dry) − 12 (hydrated with >12 H_2O),* according to Miller (2002).

For temperature modulated excitation spectroscopy two thermostats were used, one set to $T_1 = 28.6$°C, the other set to $T_2 = 28.2$°. Modulated excitation was performed by computer-controlled periodic switching of a valve, thus feeding during the first half-period water of temperature T_1 to the heat exchangers of the cell, switching to T_2 during the second half-period. The difference $\Delta T = 0.4$°C corresponds to the uncertainty of temperature control during an electric field modulated excitation. The stimulation period of the T-ME measurements was 10.68 min. Compared to the E-ME experiments this longer period was used to ensure complete heat exchange with the sample in the cell. Sixty-four sample-point spectra consisting each of 75 scans were recorded during a stimulation period and the modulation cycles were repeated until at least the same signal to noise ratio as in electric field experiments was maintained (1125 scans per sample-point spectrum at least).

Infrared spectroscopy

The measurements were performed on a Bruker IFS 66 FTIR spectrometer (Bruker Optics, Ettlingen, Germany) equipped with a liquid nitrogen cooled mercury-cadmium-telluride detector and a wire grid polarizer (0.12-μm wide Al strips on a KRS-5 substrate (SPECAC, Orpington, UK). Stationary and ME spectra were measured at two orthogonal polarizer settings. The plane of incidence is defined by the direction of light propagation and by the normal to the windows of the transmission cell in oblique position. i.e., $\varphi > 0°$. Thus pp means that the electric vector of the incident transversal wave is in this plane, whereas vp denotes the situation where the vector is orthogonal to this plane (i.e., parallel to the rotation axis of the transmission cell). Measurements were performed with pp and vp incident light and two cell positions, namely at normal incidence $\varphi = 0°$ and at oblique incidence $\varphi = 45°$. It should be noted, however, that in the latter case refraction at the sample ($n_{sample} = 1.45 \pm 0.05$) resulted in a reduced effective angle of incidence of $\varphi_{eff} = 29° \pm 3°$ as shown by Fig. 3.

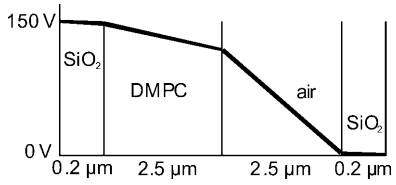

FIGURE 2 Potential profile along the path through the transmission cell. The thickness (not to scale) of each dielectric layer is indicated at the bottom. The respective potential changes were calculated by Eq. 1. The electric field in the membrane was found to be $(1.2 \pm 0.7) \cdot 10^7$ V/m. The relative large limits of uncertainty correspond to a confidence of ~95% resulting predominantly from uncertainties with respect to the lipid multilayer thickness and homogeneity. For a summary of calculated data see Table 1.

The spectrometer was permanently purged with dry and carbon-dioxide-free air. A nominal resolution of 4 cm^{-1} with zero filling factor 4 and a Blackman Harris 3 term apodization were used.

RESULTS

Stationary spectra of DMPC

Stationary spectra of DMPC multilayers measured with parallel (∥, pp) and perpendicular (⊥, vp) polarized incident light are presented in Fig. 4. Two angles of incidence, $\varphi = 0°$ and $\varphi = 45°$ were used. At normal incidence $\varphi = 0°$, both polarizations resulted in the same band intensities, thus confirming the expected isotropy of the DMPC layers with respect to the plane parallel to the cell window. Therefore, only the ⊥ spectrum is shown in Fig. 4.

The assumed ultrastructure is microcrystalline (MCU) and may be described in terms of orientation according to Fig. 5. The mean direction of the hydrocarbon chains is referred to as molecular axis ***t***. It is inclined by the angle θ_t with respect

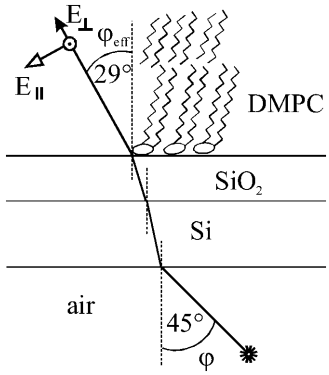

FIGURE 3 Ray tracing of the IR beam through the relevant part of the transmission cell under oblique incidence $\varphi = 45°$. In the optically dense silicon window ($n_{Si} = 3.42$) of 2-mm thickness the beam arriving at an angle of incidence of 45° is refracted significantly toward the normal. A slight opening occurs in the thin SiO_2 layer (0.2 μm, $n_{SiO2} = 2.4$) followed by a further opening in the lipid membrane region (2.5 μm, $n_{DMPC} = 1.45$). Consequently, the nominal angle of incidence of 45° is reduced by refraction to an effective angle of incidence $\varphi_{eff} = 29.3°$.

to the z-axis, which is the normal to the cell window. According to sample preparation, isotropy of the angle ϕ_t, i.e., of $\boldsymbol{t}$ around the z-axis, has to be assumed. Considering now a methylene group in a straight hydrocarbon chain, the HCH plane will be orthogonal to $\boldsymbol{t}$ and its orientation in space is determined by the angle ψ_t. The angles ϕ_t, θ_t, and ψ_t are referred to as Eulerian angles. They are used in this case to establish the relation between the unit vector of a transition moment in the molecule fixed coordinate system ($\boldsymbol{t}$-system, x_t, y_t, z_t) and the labor-coordinate system (x, y, z). For details see Fringeli et al. (2002).

Considering the symmetric stretching vibration $\nu_s(CH_2)$ at 2850 cm^{-1}, the corresponding direction of the transition moment may be assumed to be along the bisectrice of the HCH angle. Selecting this direction as x_t-axis, the unit vector $\mathbf{m_t}(\nu_s(CH_2))$ assumes the coordinates $m_{tx}(\nu_s(CH_2)) = 1$, $m_{ty}(\nu_s(CH_2)) = 0$, $m_{tz}(\nu_s(CH_2)) = 0$. Because the transition moment of the asymmetric stretching vibration $\nu_{as}(CH_2)$ at 2919 cm^{-1} is expected to be orthogonal to $\mathbf{m_t}(\nu_s(CH_2))$, i.e., $m_{tx}(\nu_{as}(CH_2)) = 0$, $m_{ty}(\nu_{as}(CH_2)) = 1$, $m_{tz}(\nu_{as}(CH_2)) = 0$.

Because primary experimental data are always related to the labor-coordinate system x, y, z, $\mathbf{m_t}$ has now to be transformed to $\mathbf{m}$, which is the unit vector of the same transition moment, but related to the labor-coordinate system according to Eq. 2.

$$\mathbf{m} = \mathbf{T}(\phi_t, \theta_t, \psi_t) \times \mathbf{m_t}, \tag{2}$$

where $\mathbf{T}(\phi_t,\theta_t,\psi_t)$ denotes the corresponding transformation matrix (Eq. 3)

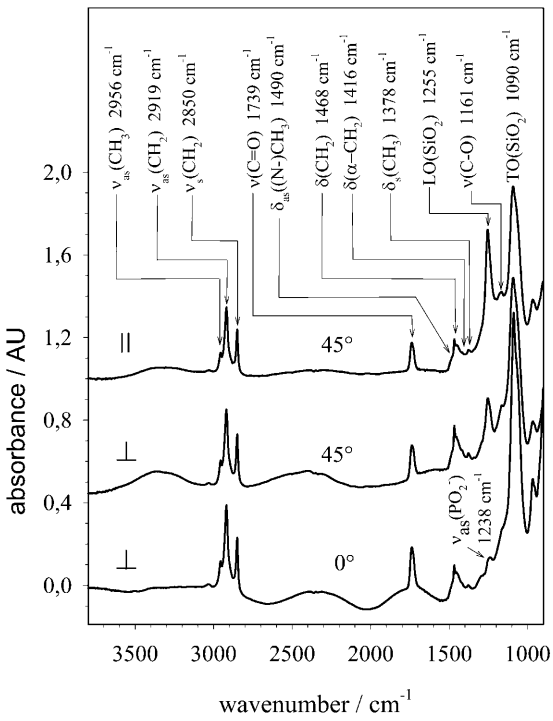

FIGURE 4 Stationary absorbance spectra of multibilayers of DMPC. Parallel (||, pp) and perpendicular (⊥, vp) polarized infrared light with angles of incidence of $\varphi = 0°$ and $\varphi = 45°$. The spectrum with parallel polarized light is practically equivalent to the spectrum with perpendicular polarized light at an angle of incidence of $\varphi = 0°$ and therefore not shown. Corresponding background spectra were recorded after displacement of the transmission cell out of the IR beam by a computer controlled shuttle.

$$T = \begin{pmatrix} \cos\psi_t\cos\phi_t - \cos\theta_t\sin\phi_t\sin\psi_t & -\sin\psi_t\cos\phi_t - \cos\theta_t\sin\phi_t\cos\psi_t & \sin\theta_t\sin\phi_t \\ \cos\psi_t\sin\phi_t + \cos\theta_t\cos\phi_t\sin\psi_t & -\sin\psi_t\sin\phi_t + \cos\theta_t\cos\phi_t\cos\psi_t & -\sin\theta_t\cos\phi_t \\ \sin\psi_t\sin\theta_t & \cos\psi_t\sin\theta_t & \cos\theta_t \end{pmatrix}. \tag{3}$$

The relative absorbance can now be calculated according to Eqs. 4 and 5.

$$A_{\parallel}^{rel} = \left(m_x \times e_{\parallel,x} + m_z \times e_{\parallel,z}\right)^2 \tag{4}$$

$$A_{\perp}^{rel} = \left(m_y \times e_{\perp,y}\right)^2, \tag{5}$$

where $e_{\parallel,x} = \cos\varphi_{eff}$, $e_{\parallel,y} = 0$ and $e_{\parallel,z} = \sin\varphi_{eff}$ denote the components of the unit vector of the parallel polarized incident electric field. φ_{eff} is the effective angle of incidence associated with the nominal tilt angle φ of the transmission cell (see Fig. 3). For normal incidence $\varphi = \varphi_{eff} = 0$. For perpendicular polarized incident light it follows $e_{\perp,x} = 0$, $e_{\perp,y} = 1$, and $e_{\perp,z} = 0$.

Orientation analysis is generally based on the evaluation of the dichroic ratio R defined by Eq. 6

$$R = \frac{A_{\parallel}^{rel}}{A_{\perp}^{rel}} = \frac{\left(m_x \times e_{\parallel,x} + m_z \times e_{\parallel,z}\right)^2}{\left(m_y \times e_{\perp,y}\right)^2}. \tag{6}$$

Equation 6 results in the dichroic ratio for a distinct molecular orientation in space. However, because our system assumes a microcrystalline ultrastructure, numerator and denominator have to be averaged over the angle ϕ_t ($0 \le \phi_t \le 2\pi$). Calculated dichroic ratios R for MCU, as a function of the angle ψ_t (rotation of CH_2-group about the molecular axis $\boldsymbol{t}$) and with the tilt angle θ_t between $\boldsymbol{t}$ and the z-axis as parameter are shown in Fig. 6 *A*. Experimentally, the dichroic ratio obtained with normally incident light, $R(\varphi = 0) = A[\nu_s(CH_2)]_{\parallel,0°} / A[\nu_s(CH_2)]_{\perp,0°} = 1.00 \pm 0.05$ thus confirming isotropic arrangement of microcrystals around the z-axis. At oblique incidence of $\varphi = 45°$, however, the dichroic ratios obtained from $\nu_s(CH_2)$ and $\nu_{as}(CH_2)$ differ significantly from the isotropic value $R^{iso} = 1$. It resulted $R(\nu_s(CH_2)) = 0.83 \pm 0.07$, and $R(\nu_{as}(CH_2)) = 0.90 \pm 0.07$. Assuming that methylene groups of the hydrocarbon chains contribute the major part to the intensities of both bands one may determine both, the mean rotation of a methylene group about the molecular axis $\boldsymbol{t}$, as well as the tilt angle of this axis

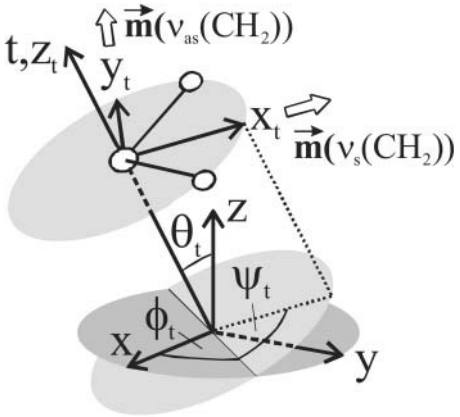

FIGURE 5 Description of the special orientation of a methylene group in a hydrocarbon chain. According to the sample preparation isotropy of the angle ϕ_t, i.e., of $\boldsymbol{t}$ around the z-axis, has to be assumed. This ultrastructure is referred to as microcrystalline ultrastructure, i.e., an isotropic arrangement of molecules around the labor-coordinate z-axis, which is the normal to the cell window whereas θ_t and ψ_t exhibit distinct values. The mean direction of the hydrocarbon chain is referred to as the molecular axis $\boldsymbol{t}$. It is inclined by the angle θ_t with respect to the z-axis. The HCH plane is orthogonal to $\boldsymbol{t}$ and its orientation in space with respect to the labor-coordinate system is determined by the Eulerian angles ϕ_t, θ_t and ψ_t. The unit vectors of the transition moments of the symmetric and asymmetric stretching vibrations of a methylene group, $\mathbf{m}(\nu_s(CH_2))$ and $\mathbf{m}(\nu_{as}(CH_2))$, are indicated as broad arrows.

with respect to the z-axis (normal to the supporting window). Thus it follows from Fig. 6 *A* that the rotation of the bisectrice of the HCH angle about the $\boldsymbol{t}$-axis results in a mean value of $\psi_t = 30° \pm 5°$ (see Fig. 5). This is also the mean direction of the transition moment of $\nu_s(CH_2)$, whereas the transition moment of $\nu_{as}(CH_2)$ is expected to be orthogonal to the latter, thus corresponding to $\psi_t = 120° \pm 5°$. Because both vibrations are related to the same molecular tilt angle of the hydrocarbon chains with respect to normal to the supporting window, it follows a chain tilt angle of $\theta_t = 35° \pm 5°$. Compared to $\theta_t = 12°$ as reported from an x-ray diffraction study of DMPC (Pearson and Pascher, 1979) our finding reflects a broad distribution of uniaxial orientations of the microcrystals formed upon evaporation of water, i.e., a significantly reduced overall ordering compared with a single crystal.

It is known that phospholipids orient spontaneously into well-ordered thin multibilayers as long as the number of bilayers does not exceed a few multiples of ten (Fringeli and Günthard, 1981). On the other hand, if the thickness of the lipid assembly is in the μm region (>100 double layers) significant loss or ordering must be taken into account, as was also the case with our DMPC preparations. The following prominent bands have turned out to be sensitive to strong electric fields (see also Fig. 4, assignments according to Fringeli and Günthard (1981)): $\nu_{as}(CH_3)$ at 2956 cm^{-1}, $\nu_{as}(CH_2)$ at 2919 cm^{-1}, $\nu_s(CH_2)$ at 2850 cm^{-1}, ν(C=O) of the two ester groups at 1739 cm^{-1}, δ_{as}((N-)CH_3), asymmetric bending of the *N*-methyl groups, as broad

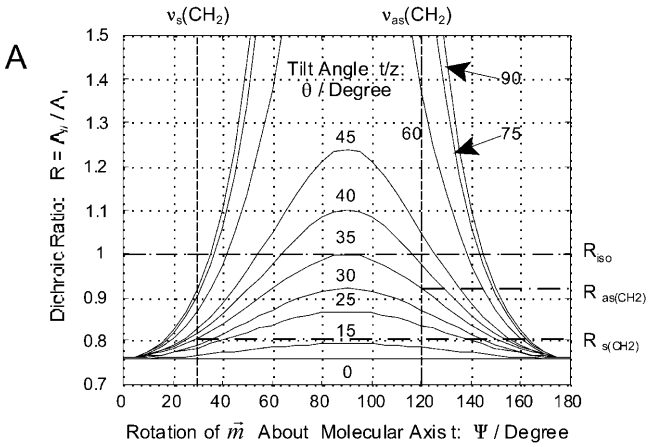

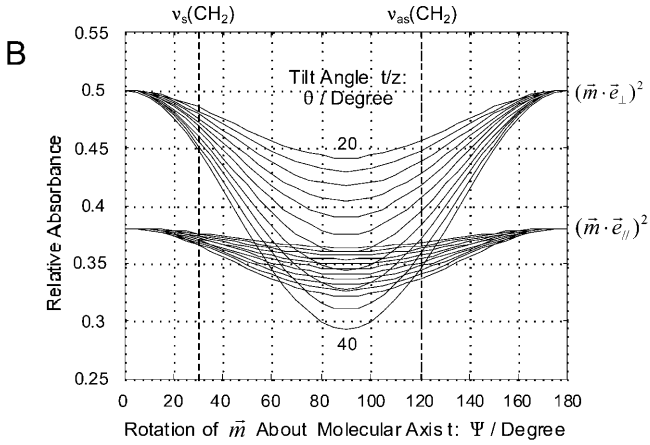

FIGURE 6 (*A*) Calculated dichroic ratio R as a function the angle ψ_t (rotation of CH_2-group about the molecular axis $\boldsymbol{t}$). The tilt angle θ_t between the $\boldsymbol{t}$ and the z-axis is used as parameter. Experimentally determined dichroic ratios of the symmetric and asymmetric methylene stretching vibrations, $R(\nu_s(CH_2)) = 0.83 \pm 0.07$, and $R(\nu_{as}(CH_2)) = 0.9 \pm 0.07$ are consistent with the finding of a mean rotation of the bisectrice of the HCH angle about the $\boldsymbol{t}$-axis of $\psi_t = 30° \pm 5°$ (see Fig. 5). This is also the mean direction of the transition moment of $\nu_s(CH_2)$, whereas the transition moment of $\nu_{as}(CH_2)$ is expected to be orthogonal to the latter, that is equivalent to $\psi_t = 120° \pm 5°$. Because both vibrations are related to the same molecular tilt angle of the hydrocarbon chains with respect to the normal to the supporting window, it follows for this angle $\theta_t = 35° \pm 5°$. The nominal tilt angle of the transmission cell with respect to the beam propagation was $\varphi = 45°$. Due to refraction (see Fig. 3) the effective tilt angle of the sample resulted in $\varphi_{eff} = 29.3°$. A microcrystalline ultrastructure (MCU) was assumed. (*B*) Calculated relative absorbance for parallel ($\parallel$) and perpendicular ($\perp$) polarized incident light entering the sample at $\varphi_{eff} = 29.3°$ (see Fig. 3). The tilt angle θ_t between $\boldsymbol{t}$ and the z-axis is used as parameter with 2° resolution between $\theta_t = 20°$ and $\theta_t = 40°$. Introducing the mean rotation angles of the transition moments of $\nu_s(CH_2)$ ($\psi_t = 30° \pm 5°$) and $\nu_{as}(CH_2)$ (($\psi_t = 120° \pm 5°$)) into the figure, one realizes that the asymmetric CH-stretching vibration is expected to be significantly more sensitive to changes of the tilt angle of the molecular axis $\boldsymbol{t}$ with respect to the z-axis. Moreover, enhancing the tilt angle of $\boldsymbol{t}$ leads to negative difference spectra in both polarizations, whereas the higher sensitivity is achieved with perpendicular polarized incident light.

shoulder near 1490 cm^{-1}. The sharp peak at 1468 cm^{-1} results from methylene bending $\delta(CH_2)$ of the hydrocarbon chains with predominantly extended (all-*trans*) chains. This peak is sitting on a broad shoulder located at ~1455 cm^{-1}, resulting from $\delta(CH_2)$ of hydrocarbon chains with *gauche* defects, and of $\delta_{as}(CH_3)$ of the hydrocarbon chains. There are two further weak but resolved bands to be mentioned, namely at 1416 cm^{-1} and 1378 cm^{-1} resulting from $\delta(\alpha\text{-}CH_2)$ of the α-methylene groups in the hydrocarbon chains, and from symmetric bending $\delta_s(CH_3)$ of the end-standing methyl groups in the hydrocarbon chains, respectively. Unfortunately, the region below 1300 cm^{-1} is strongly overlapped by vibrations of the thin SiO_2 layer. This layer served to protect the Si windows from electrochemical decomposition. As a consequence, in this setup access to typical vibrations of the polar headgroup was significantly hindered. The so-called transverse optic (TO) and longitudinal optic (LO) modes of the asymmetric Si-O stretching vibrations of the SiO_2 layer at 1090 cm^{-1} and 1255 cm^{-1}, respectively, are known to be strongly polarized (Martinet and Devine, 1995; Harbecke et al., 1985), which is also observed in our measurements. The LO mode has a transition moment perpendicular to the SiO_2 layer, i.e., it should be absent at normal incidence, which is actually the case, because the remaining band at 1238 cm^{-1} most probably results from asymmetric PO_2^- stretching $(\nu_{as}(PO_2^-))$. A further component at 1161 cm^{-1} is visible at both nominal angles of incidence, $\varphi = 0°$ and 45°, respectively. This band is associated with C-O single bond stretching ν(C-O). Finally, the band at 968 cm^{-1} may be used as a marker for the quaternary ammonium group in the polar headgroup of DMPC. It results from asymmetric stretching of $N\text{-}(CH_3)_3^+$ $(\nu_{as}(N\text{-}(CH_3)_3^+))$ vibrations. This group should be especially sensitive to electric fields due to its charge, however, overlapping with the spectrum of the SiO_2 layer disables again a reliable access.

Nearly all spectra are overlapped by broad regular bands (fringes) resulting from interference phenomena of the IR beam in the transmission cell.

Modulation spectra

The interpretation of the stationary spectra of DMPC should help to get a better understanding of the spectral changes obtained under the influence of a strong external electric field. As mentioned earlier, ME technique was applied to achieve optimum sensitivity and background compensation. For details on this less-known technique the reader is referred to Fringeli et al. (2000), Baurecht and Fringeli (2001), and Baurecht et al. (2002). A brief explanation of ME spectroscopy shall be given here for a better understanding of the interpretation of the electric field effects on DMPC. The rectangular potential applied to the sample (see Fig. 1) had a fundamental frequency of $f_m = 1.25$ Hz. In reality, rectangular excitation means multifrequency stimulation of the sample by the frequencies $(2n + 1)\,f_m$ with $n = 0, 1, 2, 3, \ldots$, where the relative amplitudes decline by the factor $1/(2n + 1)$. If a sample responds to such a stimulation, it will do it with these frequencies, and in the case of nonlinear responses also with higher harmonics of each fundamental. It is just this periodicity that renders ME techniques so sensitive, because phase-sensitive detection (PSD) may be used to separate weak periodic signals of known frequency from a huge background, which is not affected by the stimulation. PSD results in utmost signal-to-noise ratios. To understand the spectra presented in Fig. 7, it is necessary to take notice of the fact that PSD leads to output signals that can be described by the following equation:

$$A_k(\Phi_k - \Phi_{k,PSD}) = A_{k0}\cos(\Phi_k - \Phi_{k,PSD}). \qquad (7)$$

A_k and A_{k0} denote the absorbance of a so-called phase resolved spectrum and the corresponding maximum absorbance, respectively, with $k = 1, 2, 3, 4, \ldots$. $k = 1$ relates to the fundamental frequency, i.e., the linear response to the

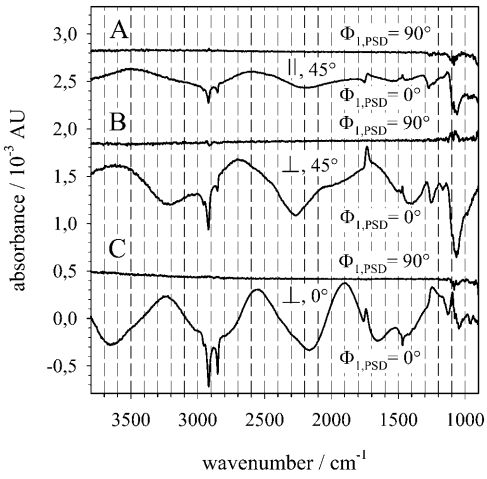

FIGURE 7 Electric field modulated excitation (E-ME) spectra of dry DMPC multibilayers detected at the fundamental frequency (1ω) and two orthogonal $\Phi_{1,PSD}$ settings, $\Phi_{1,PSD} = 0°$ and 90°, respectively. $\Phi_{1,PSD} = 0°$ results in sample responses that are in-phase with the external stimulation. The measurements were performed at two nominal angles of incidence, $\varphi = 0°$ and 45°, respectively, always with parallel (||, pp) and perpendicular (⊥, vp) polarized infrared light. $\Phi_{1,PSD} = 90°$ turned out to be that phase angle where the PSD output became zero (see Eq. 7). Consequently, $\Phi_{1,PSD} = 0°$ is an orthogonal modulation spectrum resulting in maximum amplitudes. The fact that all absorption bands of the same modulation spectrum can be set to zero ($\Phi_{1,PSD} = 90°$) indicates that the applied modulation frequency $f_m = 1.25$ Hz was too slow to produce phase shifts in the responses of different parts of the sample as well as of the electromechanically created modulated interference fringes. Therefore, all effects are nearly in-phase with the stimulating electric field. The amplitudes of modulated absorbances turned out to be only 1–2/mil of the stationary absorbance. Therefore, 3000 scans with (⊥ polarization at $\varphi = 0°$ (C) and with || polarization at $\varphi = 45°$ (*A*), as well as 6000 scans with ⊥ polarization at $\varphi = 45°$ incidence (*B*) were necessary to achieve an adequate signal-to-noise ratio. For the interpretation of the modulation spectra see text.

stimulation with frequency f_m. Φ_k denotes the phase lag of a response with frequency kf_m with respect to the stimulation. $\Phi_k = 0$ means a sample response without any delay. Each delay in a sequence of sample responses results in a contribution $\Phi_k < 0$. A sample may respond to an external stimulation by structural reorientation or chemical reaction. This case is of special interest in ME spectroscopy because it enables access to kinetic data and to the reaction scheme. Finally, $\Phi_{k,PSD}$ denotes an arbitrary angle, to be set by the operator and associated with the frequency kf_m. It follows from Eq. 7 that the PSD output signal varies within $+A_{k0}$ and $-A_{k0}$, with zero crossings at $(\Phi_k - \Phi_{k,PSD}) = 90°$ and 270°. Obviously, the operator has the possibility to sense the phase of a signal response by choosing adequate settings of $\Phi_{k,PSD}$. Modulation spectra obtained at two values of $\Phi_{k,PSD}$ differing by 90°, so-called orthogonal modulation spectra, are required to get time-resolved information about the stimulated process. Finally, it should be mentioned once more, that PSD cancels all parts of the overall spectrum that do not contain periodic absorbance changes with frequencies of kf_m.

The spectra shown in Fig. 7 are overlapped by wavelike signals, that result from interferences produced by a periodic change of the distance between the windows as a consequence of the applied high periodic potential. According to Eq. 7 there must exist a phase setting $\Phi_{1,PSD}$ that cancels this perturbation. This is the case at $\Phi_{1,PSD} = 90°$, however, as shown by Fig. 7, all other signals vanished at this setting, too. Thus one can conclude that there is no phase difference $\Delta\Phi_1$ between the mechanical response of the cell and the field-induced effects in the sample; both react without delay to the external stimulation. Consequently, both contributions reach maxima or minima at $\Phi_{1,PSD} = 90° - 90° = 0°$, meaning that the disturbance by fringes cannot be traced by setting an adequate $\Phi_{1,PSD}$. We conclude that the largest relaxation time of our system was still considerably shorter than the period of our stimulation, which was $\tau = 0.8$ s (see also Fig. 8 legend). Consequently, ME spectroscopy was reduced in this case to a high-performance difference spectroscopy, which enabled unambiguously the detection of specific parts of the DMPC molecule that responded periodically to the external field stimulation. These group vibrations were: $\nu_{as}(CH_3)$, $\nu_{as}(CH_2)$, $\nu_s(CH_2)$, ν(C=O), $\delta(CH_2)$, $\delta_s(CH_3)$, $\nu_{as}(PO_2^-)$, $\nu_s(PO_2^-)$, ν(C-O), and $\nu_{as}(\text{N-}(CH_3)_3^+)$. Quite obviously, the whole molecule was affected by the externally applied electric field. This is contradictory to the finding by Le Saux et al. (2001), who reported conformational changes to occur only in the polar headgroup.

The modulation spectra shown in Fig. 7 feature positive and negative, as well as sigmoidal bands, depending on the angle of incidence φ, and on the polarization. Considering first normal incidence, i.e., $\varphi = 0°$, there are negative bands resulting from typical vibrations of the CH_2 and CH_3 groups of the hydrocarbon chains as assigned earlier, as well as of

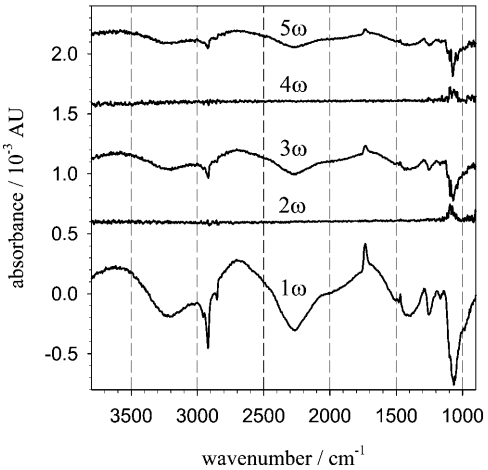

FIGURE 8 Phase sensitive detection up to 5ω of the spectroscopic response of dry DMPC multilayers to a rectangular stimulation by an electric potential, switching between +150 V and 0 V. Angular frequency of fundamental $\omega = 2\pi f_m = 7.85\,s^{-1}$. The amplitudes of odd multiples of the fundamental frequency behave like 1:1/3:1/5:... compared to the fundamental, thus reflecting a nondamped response to the rectangular stimulation. Consequently, the slowest stimulated process in the DMPC layers exhibits a relaxation time $\tau_{max} \ll 1/(5\omega) = 25.5$ ms. The absence of any modulated sample responses at 2ω and 4ω demodulation frequency indicates a strict linearity of the stimulated process. The phase resolved spectrum at the fundamental frequency 1ω is the same as shown in Fig 7 *B*. For experimental details see legend to Fig. 7.

$\nu_{as}(\text{N-}(CH_3)_3^+)$. Positive bands are resulting from $\nu_{as}(PO_2^-)$ and ν(C-O) of the ester groups. There is also a distinct positive band at 1095 cm^{-1}, which tentatively is assigned to $\nu_s(PO_2^-)$, however, it should be mentioned that in this spectral region there is significant uncertainty due to the proximity to the TO mode of SiO_2. On the other hand, the 1095 cm^{-1} band is also visible as shoulder in both polarizations at $\varphi = 45°$ incidence. ν(C=O) exhibits a distinct sigmoidal shape. In the stationary spectra shown in Fig. 4, ν(C=O) is located at 1738 cm^{-1} in all cases. In the modulation spectra, however, we find minima and maxima of the sigmoidal shape depending significantly on the angle of incidence and the polarization as well. For $\varphi = 0°$ they were located at 1761 cm^{-1} and 1741 cm^{-1}, i.e., significantly above the position in the field-free state. Similar observations are made at oblique incidence $\varphi = 45°$. For parallel ($\parallel$) polarized incident light the minimum and maximum are found at 1752 cm^{-1} and 1730 cm^{-1}, respectively, whereas for perpendicular ($\perp$) polarized incident light minimum and maximum are found at 1755 cm^{-1} and 1733 cm^{-1}, respectively. No definite interpretation can be given at the moment, however, concerning the sign of a band, one can state that a positive sign in the $\Phi_{1,PSD} = 0°$ spectrum means that the average transition dipole moment was deflected by the stimulating electric field toward the incident infrared electric field vector, whereas the opposite deflection would result in a negative band in the modulation spectrum. A more distinct picture of the field induced process in the membrane

can be derived from Fig. 6 *B* where the relative absorbance of $\nu_s(CH_2)$ and $\nu_{as}(CH_2)$ were calculated as a function of the angle ψ_t, i.e., the angle of rotation of the molecule fixed coordinate system about the molecular axis $\boldsymbol{t}$. The molecular tilt angle θ_t was considered as parameter, varying between 20° and 40° in steps of 2°. If the sample is set to oblique incidence ($\varphi = 45°$ nominal, $\varphi_{eff} = 29.3°$ effective; see Fig. 3), it follows from Fig. 6 *B* that perpendicular polarized light is significantly stronger absorbed and also stronger dependent on the tilt angle θ_t. Directing now the unit vector of the transition moment of $\nu_s(CH_2)$ along the x_t-axis and that of $\nu_{as}(CH_2)$ along the y_t-axis, as shown in Fig. 5, it is quite evident from Fig. 6 *B* that in a general setting of ψ_t, $\nu_s(CH_2)$ and $\nu_{as}(CH_2)$ will exhibit a different sensitivity to changes of the tilt angle θ_t. Only in case of $\psi_t = 45°$ both react in the same way. Taking into account the finding that mean values of rotation and tilting assumed $\psi_t = 30°$ and $\theta_t = 35°$ (see legends for Figs. 4 and 6 *A*), it follows immediately from Fig. 6 *B* that the enhancement of the tilt angle will result in negative difference bands for both, $\nu_s(CH_2)$ and $\nu_{as}(CH_2)$. Moreover, the effect will be more distinct by a factor of ~3, with perpendicular polarized light. Finally, with $\psi_t = 30°$, the difference band resulting from $\nu_{as}(CH_2)$ is expected to be ~3–4 times more intense than the corresponding difference band associated with $\nu_s(CH_2)$. This is exactly what is observed in the E-ME spectra at oblique incidence, Fig. 7, *A* and *B*. Therefore, we conclude that the compression of dry DMPC bilayer by a strong electric is accomplished by a reversible enhancement of the tilt angle θ_t. Thus E-ME modulates this angle about the mean value $\theta_t = 35°$ with an amplitude $\Delta\theta_t$ that must be expected to be very small, because the corresponding absorbance is found to be in the range of 20–400 μAU.

Influence of modulated temperature to DMPC

Our experimental setup enabled a temperature control to ±0.2°C. Therefore the question arose whether the detected modulated response of DMPC could not result from a modulated current <1 pA, i.e., smaller than our detection limit, across the sample and thus leading to a periodic heating.

There are two convincing arguments against temperature modulated excitation:

1. As already mentioned earlier, a rectangular stimulation with frequency ω as applied in this case leads to a synchronous stimulation of frequencies $(2n + 1)\,\omega$ with $n = 0, 1, 2, 3\ldots$. According to the Fourier analysis an amplitude damping of $1/(2n + 1)$ is expected. The PSD of higher harmonics is automatically performed by digital methods (Fringeli, 1997; Baurecht and Fringeli, 2001). Modulation spectra obtained by demodulating the sample response at frequencies 1–5ω is shown as an example in Fig. 8. Demodulation with the fundamental frequency ω leads to the spectrum already shown in Fig. 7 *B*. Demodulation by 2ω and 4ω resulted in flat baselines over the entire spectrum, however, demodulation with 3ω and 5ω resulted in similar spectra to the 1ω-demodulation downscaled by 1/3 and 1/5, respectively. As a consequence, DMPC responded to the rectangular electric field stimulation as linear system. Moreover, no phase lag could be detected in the response to 5ω, corresponding to a frequency of 6.25 Hz, meaning that the stimulated process must have relaxation times significantly smaller than $1/5\omega = 25.5$ ms. This observation implies that the sample reacted completely reversible to the external stimulation in a millisecond timescale. Because the transmission cell in use exhibited a time constant in the minute range for heat exchange, it would never be possible to dissipate electrically produced heat in the sample within ≤25.5 ms, thus disabling 0° phase lag up to 5ω as obtained by electric field modulation as shown in Fig. 8.
2. Nevertheless we wanted to know what T-ME spectra look like, when the sample is stimulated around the mean temperature of $T = 28.4$°C with an amplitude of 0.2°C, corresponding to the limit of confidence of the temperature control system. T-ME was exerted to the sample by switching the water flow through the heat exchanger plates of the transmission cell periodically between two thermostat baths held at 28.6°C and 28.2°C, respectively. To establish nearly complete heat exchange in the cell, the stimulation period had to be extended considerably from $T_m = 0.8$ s in the case of E-ME to $T_m = 10.68$ min for T-ME. As shown by Fig. 9, sample responses appear in both channels, $\Phi_{1,PSD} = 0°$ and $\Phi_{1,PSD} = 90°$ indicating still a significant phase lag of the response with respect to the onset of temperature rise. This phase lag result from two sequential processes, heat transfer and the kinetics of temperature-induced conformational changes, whereas only the latter contributes to the spectral shape. $\Phi_{1,PSD}$ is under the control of the operator and therefore, according to Eq. 7 the variation of $\Phi_{1,PSD}$ between 0 and 2π renders phase-resolved modulation bands that move once through a maximum and a minimum. Zero crossing between them is easiest to be detected experimentally, corresponding to $\Phi_{1,i} - \Phi_{1,PSD} = \pm 90°$. Thus the phase lag introduced by the system results in $\Phi_{1,i} = \Phi_{1,PSD} \pm 90°$ (zero crossing). Time resolution in modulation spectroscopy means that there are parts in the system resulting in modulation bands with different phase lags. To achieve this situation the stimulation frequency has to be adapted to the relaxation constants of the system in such a way that $0.1 < \omega \times \tau < 10$ where τ is a relaxation constant of the system (Fringeli et al., 2000). Considering, for example, the orthogonal modulation spectra obtained at normal light incidence $\varphi = 0°$ (Fig. 9 *C*) one realizes that the two spectra are not completely similar, i.e., may be converted

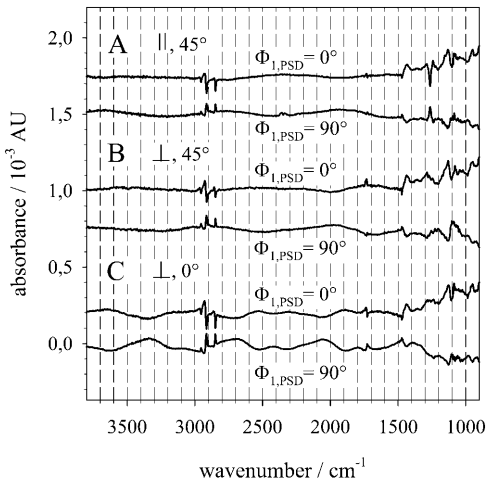

FIGURE 9 Temperature-modulated excitation spectra of dry DMPC multibilayers detected at the fundamental frequency (1ω) and two orthogonal $\Phi_{1,PSD}$ settings, $\Phi_{1,PSD} = 0°$ and 90°, respectively. $\Phi_{1,PSD} = 0°$ results in sample responses that are in-phase with the external stimulation. The measurements were performed at two nominal angles of incidence, $\varphi = 0°$ and 45°, respectively, always with parallel (||, pp) and perpendicular ($\perp$, vp) polarized infrared light. Due to the slow heat exchange in the transmission cell the modulation period had to be extended from 0.8 s in case of E-ME to 10.68 min for T-ME. The temperature was modulated by ± 0.2° around the mean value of 28.4°C, i.e., just within the range of uncertainty of the temperature control. Most significantly, compared to E-ME (Figs. 7 and 8), T-ME results in modulation spectra of similar magnitude, however, with completely different shapes, proving unambiguously that E-ME spectra are not ''contaminated'' by temperature effects resulting from modulated Joule heating. Even in this very narrow temperature range, T-ME spectra feature the typical effects of hydrocarbon chain melting, influencing also the structure of the polar headgroups. See text for details.

into each other by a simple factor. In the CH-stretching region a phase difference of 10° ± 2° were evaluated from the determination of the corresponding PSD phase settings to reach zero crossing. As a consequence, the relaxation constant of the temperature-induced conformational changes in the hydrocarbon chain region of dry DMPC multilayers may be estimated to be in the range of $\tau_T = 2$ min. In the case of E-ME, however, it was found from the 5ω-spectrum in Fig. 8 that $\tau_E \ll 25$ ms. Thus it can be concluded unambiguously that T-ME and E-ME to dry DMPC resulted in quite different responses. This conclusion is most evidently supported by visual comparison of E-ME (Fig. 7) and T-ME (Fig. 9) spectra.

Interpretation of the electric field effect on a molecular level

As to be concluded from the spectral behavior of CH-stretching vibrations, T-ME results in reversible *gauche* defects in the hydrocarbon chains (Hübner and Mantsch, 1991). On the other hand CH-stretching bands in the E-ME spectra give no evidence for such a conclusion. Electrostriction was suggested based on capacitance measurements of supported lipid membranes (Hianik, 2000; Hianik et al., 2000; Hianik and Passechnik, 1995). To check the consistence of our experimental data and interpretation with results obtained by capacitance measurements, we have calculated the Young's elasticity modulus a DMPC bilayer. The result may be compared with a number of published data in a review article by Hianik (2000).

Access to Young's modulus from E-ME data is straightforward and will be summarized as follows. Attention was made to the error propagation, aiming to indicate limits reflecting a statistical confidence of ~90%.

First the degree ρ_E of E-ME was determined by calculating the ratio of the absorbances of $\nu_{as}(CH_2)$ in the E-ME spectrum (Fig. 7, $\varphi = 0°$) and in the stationary spectrum (Fig. 4, $\varphi = 0°$), resulting in $\rho_E = 1.41 \times 10^{-3} \pm 1.34 \times 10^{-4}$. From the calculation of the relative absorbance of $\nu_{as}(CH_2)$ at normal incidence ($\varphi = 0°$) as depending on the mean values of rotation and tilting $\psi_t = 30°$ and $\theta_t = 35°$, respectively, it followed that the E-field induced modulated tilt angle resulted in $\Delta\theta_t = 0.09° \pm 0.015°$. This result enables now the calculation of the thickness variation Δz under the influence of E-ME. Taking for the length of two extended DMPC molecules in the crystal $L = 5.5$ nm (Pearson and Pascher, 1979) with an estimated uncertainty of $\Delta L = 5.5$ nm ± 0.5 nm and $\theta_t = 35° \pm 5°$ for the stationary tilt angle, it follows for the membrane thickness $d = 4.5$ nm ± 0.5 nm, and for change in membrane thickness $\Delta z = -0.0054 \pm 0.0017$ nm. To calculate the modulated pressure Δp exerted by the E-field, one may use Eq. 8, which holds for a plate condenser and thus corresponds to the equivalent circuit used earlier to calculate the electric field in the DMPC layer (see Table 1).

$$\Delta p = \frac{1}{2} \times \varepsilon_r \times \varepsilon_0 \times E^2. \tag{8}$$

Where ε_r and E denote relative permittivity and electric field in the DMPC to be introduced from Table 1, and ε_0 is the permittivity of vacuum ($\varepsilon_0 = 8.854 \times 10^{-12}$ C/(Vm)). The result is $\Delta p = 2.5 \times 10^3$ Pa ± 2.0×10^3 Pa. The large error results from the accumulation of preceding uncertainties, especially the electrostatic parameters associated with the DMPC assembly. Nevertheless, these results enable the estimation of the Young's elasticity modulus $E_\perp$ of a dry DMPC bilayer according to Eq. 9

$$E_\perp = -d \times \frac{\Delta p}{\Delta z}, \tag{9}$$

where d, Δp, and Δz denote membrane thickness, E-field induced pressure and pressure induced change of membrane thickness (Hianik and Passechnik, 1995). Introducing our data into Eq. 9 results in for the Young's modulus $E_\perp = 2.2 \times 10^6$ Pa ± 1.8×10^6 Pa. Despite the large statistical error, one can conclude that the magnitude is correct (Hianik,

2000) and that the interpretation of E-field induced hydrocarbon chain tilting is reasonable.

DISCUSSION

The influence of an electric field of the order of 10^7 V/m on the structure of dry multilayers of DMPC was studied by transmission electric field modulated excitation (E-ME) FTIR spectroscopy. The multilayers were supported on a silicon window that was coated by a thin insulating SiO_2 layer (Fig. 1). Significant spectral responses were detected in the hydrocarbon chain and fatty acid ester regions, as well as in the polar headgroup. The spectral region of the latter, however, was heavily overlapped by intense absorption bands of the SiO_2 layer. Moreover, strong interference fringes caused partial band distortions. All spectra were measured with polarized light at normal incidence and 45° inclination of the cell as shown in Fig. 4, where an assignment of relevant absorption bands is given. E-ME led to the spectra shown in Fig. 7. The fact that interference fringes are still present results most probably from a modulation of the distance between the Si cell windows by electrostatic attraction. This force is not directly exerted to the DMPC multilayers because they were separated by an air gap from the opposite window as shown by Figs. 1 and 2. However, pressure due to the high electric field across the multibilayers will also be exerted to DMPC. Conformational changes in membranes and electrostriction due to such effects have been reported from membrane capacitance measurements by Sargent (1975a,b), Hianik and Passechnik (1995), Hianik (2000), and Hianik et al. (2000). In the latter two cases solid supported membranes have been used that were quite similar to ours.

Because interference of temperature effects from periodic Joule heating of the sample by E-ME can unambiguously be excluded, as revealed by T-ME spectra shown in Fig. 9 the E-ME spectra shown in Figs. 7 and 8 reflect pure electric field induced effects. Although T-ME spectra measured in the very narrow temperature range of 28.4° ± 0.2° already show the typical phenomena of chain melting, E-ME spectra look quite different, in a first view even unrealistic, because CH_2 stretching vibrations appear in all E-ME spectra as negative bands, indicating a decrease of substance. Moreover, there is no evidence of conformational changes in the hydrocarbon chain region, as observed in the T-ME spectra, where the sigmoidal shapes of the CH_2 stretching bands indicate that a small amount of all-*trans* hydrocarbon chains are reversibly converted into chains containing *gauche* defects upon temperature increase (Hübner and Mantsch, 1991). The most probable explanation for the reaction mechanism in case of E-ME is therefore a periodic, reversible increase of the chain tilt angle under the influence of the electric field. This explanation is supported by a semiquantitative analysis of the observed dichroic phenomena. Increasing the tilt angle leads to a thinner membrane and might correspond to what was found by capacitance measurements (Hianik, 2000; Hianik et al., 2000). E-ME measurements as described in this paper can be used for an experimental determination of Young's elasticity modulus $E_\perp$. Despite the relatively large uncertainties of our basic data, the magnitude of $E_\perp$ ($E_\perp = 2.2 \times 10^6$ Pa ± 1.8×10^6 Pa) was found to be consistent with data published by Hianik (2000). This fact can be considered as a verification of the minute changes in the tilt angle ($\Delta\theta_t = 0.09° \pm 0.015°$) and membrane thickness ($\Delta z = 0.0054 \pm 0.0017$ nm) as derived from E-ME spectra.

In contrast to T-ME, E-ME results in significant effects in the fatty acid ester region around 1740 cm^{-1}. Here distinct sigmoidal band shapes can be observed indicating probably reversible conformational changes in this region induced by the change of the tilt angle of the hydrocarbon chains. Modeling of the dichroic behavior of C=O stretching band and of other absorption bands of the polar headgroup are in progress.

Moreover, we intend to apply corresponding potentials to oriented monolayers of porin Omp32 on a germanium ATR crystal in aqueous environment (Schwarzott et al., 2003) to get insight into molecular details of voltage gating. In this case, low voltage potentials (<1 V) must be used, however, high electric fields are expected in the range and under the influence of the Gouy-Chapman layer.

Finally, it should be mentioned that electric fields of the magnitude of 10^7 V/m are able to induce only very small orientational and conformational changes in supported dry lipid bilayer assemblies. In case of DMPC, as reported in this paper, the use of E-ME technique was a prerequisite to achieve the sensitivity required for the detection of the lipid response.

REFERENCES

Baurecht, D., I. Porth, and U. P. Fringeli. 2002. A new method of phase sensitive detection in modulation spectroscopy applied to temperature induced folding and unfolding of RNase A. *Vib. Spectrosc.* 30:85–92.

Baurecht, D., and U. P. Fringeli. 2001. Quantitative modulated excitation Fourier transform infrared spectroscopy. *Rev. Sci. Instrum.* 72: 3782–3792.

Fringeli, U. P., D. Baurecht, M. Siam, G. Reiter, M. Schwarzott, T. Bürgi, and P. Brüesch. 2002. ATR spectroscopy of thin films. *In* Handbook of Thin Films Materials, Vol 2, Chapter 4. H. S. Nalwa, editor. Academic Press: New York. 191–229.

Fringeli, U. P., D. Baurecht, and Hs. H. Günthard. 2000. Biophysical infrared modulation spectroscopy. *In* Infrared and Raman Spectroscopy of Biological Materials. H. U. Gremlich and B. Yan, editors. Marcel Dekker, New York. 143–192.

Fringeli, U. P. 1997. Verfahren zur simultanen, digitalen phasenempfindlichen Detektion von zeitaufgelösten, quasi-gleichzeitig erfassten Datenarrays eines periodisch stimulierten Systems. International Patent Publication, PCT, WO 97/08598, Bern, Switzerland.

Fringeli, U. P., and Hs. H. Günthard. 1981. Infrared membrane spectroscopy. *In* Molecular Biology Biochemistry and Biophysics 31 (Membrane Spectroscopy). E. Grell, editor. Springer Verlag Berlin, Heidelberg, New York. 270–332.

Robert, C. W. Handbook of Chemistry and Physics 1974–1975, 55th ed. C. W. Robert, editor. CRC Press, Cleveland, Ohio. E–58.

Harbecke, B., B. Heinz, and P. Grosse. 1985. Optical properties of thin films and the Berreman effect. *Appl. Phys. A.* 38:263–267.

Hianik, T. 2000. Electrostriction and dynamics of solid supported lipid films. *J. Biotechnol.* 74:189–205.

Hianik, T., M. Fajkus, B. Tarus, P. T. Frangopol, V. S. Markin, and D. F. Landers. 2000. The changes in dynamics of solid supported lipid films following hybridization of short sequences DNA. *Electroanalysis.* 12:495–501.

Hianik, T., and V. I. Passechnik. 1995. Bilayer Lipid Membranes: Structure and Mechanical Properties. Kluwer Academic Publishers, Dordrecht, Boston, London.

Hübner, W., and H. M. Mantsch. 1991. Orientation of specifically $^{13}C{=}O$ labelled phosphatidylcholine multilayers from polarized attenuated total reflection FT-IR spectroscopy. *Biophys. J.* 59:1261–1272.

Le Saux, A., J.-M. Ruysschaert, and E. Goormaghtigh. 2001. Membrane molecule reorientation in an electric field recorded by attenuated total reflection Fourier transform infrared spectroscopy. *Biophys. J.* 80: 324–330.

Martinet, C., and R. A. B. Devine. 1995. Analysis of the vibrational mode spectra of amorphous SiO_2 films. *J. Appl. Phys.* 77:4343–4348.

Miller, I. R. 2002. Effect of electric fields on the structure of phosphatidyl choline in a multibilayer system. *Bioelectrochemistry.* 57:145–148.

Pearson, R. H., and I. Pascher. 1979. The molecular structure of lecithin dehydrate. *Nature.* 281:499–501.

Sargent, D. F. 2001. Influence of transmembrane voltage on the structure of membrane components. *Biophys. J.* 81:1823–1824.

Sargent, D. F. 1975a. Voltage jump/capacitance relaxation studies of bilayer structure and dynamics. *J. Membr. Biol.* 23:227–247.

Sargent, D. F. 1975b. Bilayer dynamics studies using capacitance relaxation. *In* Molecular Aspects of Membrane Phenomena. H. R. Kaback, H. Neurath, G. K. Radda, R. Schwyzer, and W. R. Wiley, editors. Springer Verlag, Berlin. 104–120.

Schwarzott, M., H. Engelhardt, T. Klühspies, D. Baurecht, D. Naumann, and U. P. Fringeli. 2003. In situ FTIR ATR spectroscopy of the preparation of an oriented monomolecular film of porin Omp32 on an internal reflecting element bydialysis. *Langmuir.* 19:7451–7459.

Winterthaler, M. 1999. On the defect growth after short electric field pulses in planar lipid bilayers. *Colloids Surfaces A.* 149:161–169.